Materials Advances

ROYAL SOCIETY OF CHEMISTRY

PAPER

View Article Online
View Journal | View Issue

Cite this: *Mater. Adv.*, 2022, 3, 7946

In vitro evaluation of the biodegradability of chitosan–genipin hydrogels†

Sophie L. Reay, *[a] Emma L. Jackson,[b] Ana M. Ferreira,[a] Catharien M. U. Hilkens[b] and Katarina Novakovic[a]

Biomaterials intended for *in vivo* applications should ideally be biodegradable to prevent their retention in the body, while avoiding the need for surgical removal. This study investigates the *in vitro* lysozyme degradation of chitosan–genipin hydrogels using fluorescence formed during the crosslinking reaction between chitosan and genipin, resulting from highly conjugated heterocyclic structures. Fluorescence degradation studies showed that the supernatant of degraded hydrogels significantly fluoresced, suggesting that although the hydrogel structure was broken down, chitosan–genipin crosslinks prevail. Further studies employing FTIR showed that this is not entirely the case, and that one of the bifunctional crosslinks between chitosan and genipin is broken. Results suggest that lysozyme degrades the secondary amide linkage, whilst the tertiary aromatic amine linkage remains unbroken. Seeking to evaluate feasibility and likely mechanism of removal of degraded hydrogels *in vivo*, degraded particle size was measured. Results show existence of particles as small as 1.7 nm, which is below the threshold for renal filtration. At the same time clusters of larger particles with a mean diameter of 218.4 μm ± 17.8 were detected and shown to likely form *via* agglomeration, rather than incomplete degradation. Collectively, our findings show that lysozyme partially degrades chemical crosslinks in chitosan–genipin hydrogels, and that these hydrogels have potential to be eliminated from the body *via* urinary excretion.

Received 13th May 2022,
Accepted 23rd August 2022

DOI: 10.1039/d2ma00536k

rsc.li/materials-advances

1 Introduction

Hydrogels are three-dimensional networks of crosslinked hydrophilic polymers, primarily consisting of water.[1–3] The ability of hydrogels to absorb water is due to hydrophilic functional groups attached to the polymeric backbone, however, the crosslinks between the network chains renders hydrogels insoluble.[4] Due to their high water content and close resemblance to living tissue, hydrogels are researched in biomedicine for diverse applications including tissue engineering scaffolds and drug delivery systems.

The subject of this study are the increasingly popular chitosan-based hydrogels which, based on chitosan's properties, are deemed biocompatible and biodegradable, envisioning *in vivo* applications with minimal toxicity and natural excretion from the body.[5] In particular, the study focuses on degradability of chitosan–genipin hydrogels which, due to their chemically crosslinked structure, deviates from native chitosan molecules and requires investigation. Chitosan is a cationic, linear copolymer composed of randomly distributed β-(1,4)-linked *N*-acetyl-D-glucosamine and D-glucosamine units[6] that is produced from deacetylation of chitin (Fig. 1), which is derived from the exoskeleton of arthropods and fungal cell walls. Importantly, chitosan-based products are seen as an opportunity to fulfil zero waste economy principles, utilising chitin which is abundant in seafood waste, promoting sustainable manufacturing.

Chitosan hydrogels can be formed by both physical and chemical crosslinking. Physically crosslinked hydrogels are formed by reversible ionic interactions, hydrogen bonds, hydrophobic interactions and polymer chain entanglements.[2,4] Although they offer advantages including ease of synthesis and absence of potentially toxic crosslinking agents, their use in biomaterials can be limited due to the reversible and weak bonds, resulting in unstable hydrogels with inadequate mechanical strength.[11] On the other hand, chemical crosslinking is achieved through stronger, covalent bonds. In the case of chitosan hydrogels, crosslinking reagents including glutaraldehyde and formaldehyde form covalent bonds with the amino groups of chitosan. While efficient, these crosslinking agents enhance the toxicity of the resulting materials which is undesirable. Therefore, focus has recently shifted to the use of the bio-safe crosslinker, genipin, which is the crosslinking agent used in this study. Genipin is a natural extract from the *Gardenia jasminoides Ellis* fruit, which is widely used

[a] *School of Engineering, Newcastle University, Newcastle Upon Tyne, UK. E-mail: S.Reay2@newcastle.ac.uk*
[b] *Translational & Clinical Research Institute, Newcastle University, UK*

† Electronic supplementary information (ESI) available. See DOI: https://doi.org/10.1039/d2ma00536k

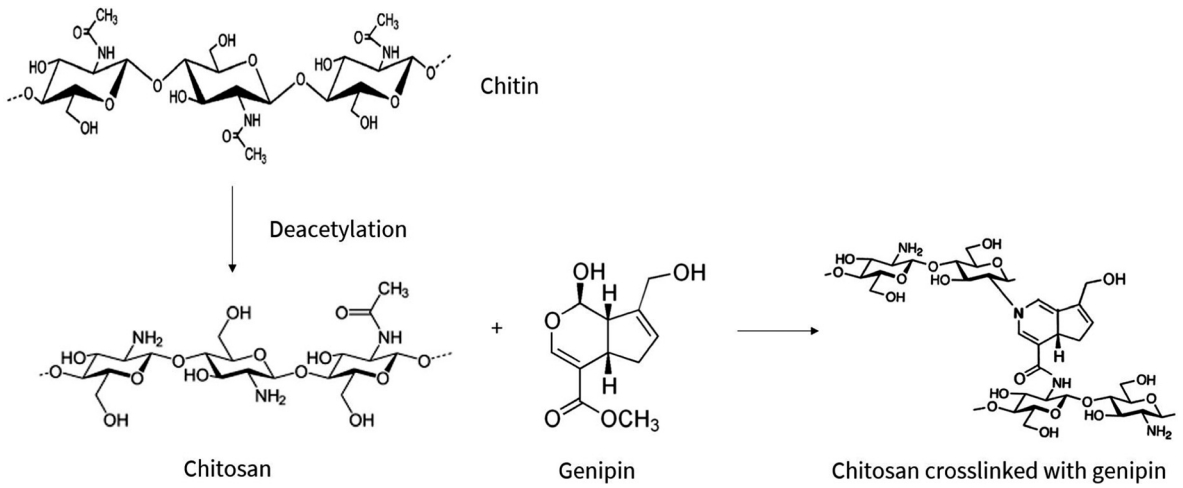

Fig. 1 Chemical conversion of chitin to chitosan *via* deacetylation process, followed by the chemical crosslinking reaction between chitosan and genipin. Adopted from ref. 7 and 8–10.

as a herbal medicine and food pigment.[4] Not only is genipin 5000–10 000 times less cytotoxic than glutaraldehyde,[12] but it also has a slower degradation rate.[13]

Genipin forms bifunctional crosslinks with chitosan molecules (Fig. 1), yielding blue-coloured, fluorescent hydrogels.[4,7,14,15] The proposed mechanism of the crosslinking reaction between chitosan and genipin is illustrated in Fig. S1 (ESI†). First, a primary amine group from a chitosan molecule drives a nucleophilic attack on the genipin olefinic carbon atom at C-3, resulting in the opening of the dihydropyran ring and the formation of a nitrogen–iridoid, which undergoes dehydration to produce aromatic intermediates. Radical-induced polymerisation of two amino-attached rings subsequently occurs, creating highly conjugated heterocyclic genipin derivatives, resulting in fluorescence. Secondary amide linkages are also established by the reaction of the ester group in genipin with the amino group in chitosan.[15,16]

For any biomaterial intended for *in vivo* use, surgical removal or decomposition is required to prevent retention in the body. In the human body chitosan is mainly degraded by lysozyme, which is detected in bodily secretions including tears, saliva, and serum.[17] Lysozyme is secreted by many glands including the lacrimal, parotid, mammary, oesophageal and bronchial glands, and is produced by cells such as monocytes, macrophages and neutrophils.[18–20] Three human chitinases, of the glycoside hydrolase family 18, with enzymatic activity have also been identified.[21] Lysozyme primarily functions as an antimicrobial agent by hydrolysing the β-(1,4) linkages between *N*-acetylmuramic acid (NAM) and *N*-acetylglucosamine (NAG) in the peptidoglycan wall of Gram-positive bacteria.[22,23] Lysozyme contains a hexametric active site containing six subsites (A–F) that bind to alternating NAG and NAM. Optimal fit of the substrate requires a steric distortion of the sugar at subsite D into the higher energy half chair conformation, thereby weakening the glycosidic bond located between sugar residues on subsites D and E.[24] The catalytic residue glutamic acid 35 (Glu35) donates a proton to the glycosidic oxygen, leading to bond cleavage and formation of a positively charged carbonium ion. Aspartate 52 acts as a nucleophile to generate a covalent glycosyl–enzyme intermediate. Glu35 then reacts with a molecule of water to form hydroxyl ion, which subsequently attacks the glycosyl–enzyme intermediate to yield the hydrolysed saccharide and the enzyme unchanged (Fig. S2, ESI†).[25] It is postulated that lysozyme degrades chitosan using a similar mechanism. Lysozyme only interacts with the acetylated units of chitosan,[26,27] thus lysozyme digestibility increases with degree of acetylation.[28–31]

To our knowledge, it has not been reported if lysozyme beaks the crosslinks between chitosan and genipin in chitosan–genipin hydrogels. If chitosan–genipin crosslinks remain intact, and degraded particles are too large to be eliminated from the body, it could result in long-term retention. Although genipin is less cytotoxic than other covalent crosslinkers, it can induce apoptosis *via* reactive oxygen species production,[16] and can react with free amino groups of amino acids within biological tissue. Furthermore, if the chitosan–genipin complex cannot be cleared by the body, it may elicit the foreign body reaction, resulting in the formation of a foreign body granuloma. In the presented work, chitosan–genipin hydrogels are enzymatically degraded with lysozyme. Fluorescence spectroscopy and Fourier-transform infrared spectroscopy are used to monitor changes in fluorescence and functional groups, respectively, to determine if chitosan–genipin hydrogels are completely biodegradable. In addition, the size of degraded particles is measured using both laser diffraction and dynamic light scattering to predict *in vivo* elimination.

2 Experimental section

2.1 Materials

Chitosan (medium molecular weight 190 000–300 000 g mol^{-1}, 75–85% deacetylation, product code 448877, lot number STBG5137V), glacial acetic acid (product code 27225-M, lot number STBH0491), genipin (≥98%, product code G4796, lot

number 0000111438), lysozyme from chicken egg white (≥90%, ≥40 000 units per mg protein, product code L6876, lot number SLCF6129) and Gibco™ PBS tablets (product number 18912014, lot number 2321011) were supplied from Sigma-Aldrich (United Kingdom).

2.2 Synthesis of hydrogels

2.2.1 Hydrogel disks. 1.5% weight by volume (w/v) chitosan solution was prepared by dissolving chitosan powder in 1% volume by volume (v/v) acetic acid solution. The solution was stirred with a magnetic stirrer in a sealed vessel for 24 hours to obtain a pale yellow, viscous solution. Both 0.5 and 1% w/v genipin solutions were prepared by dissolving genipin powder in deionised water, and used as defined in Table 1. Gelation occurred in sealed cylindrical polyethylene vials (15 mm diameter) in a Clifton oven at 37 °C for 24 hours. Upon formation, hydrogels were removed from the vials by cutting off the bottom and gently pushing the hydrogels out using a glass rod. A schematic diagram of the chitosan–genipin hydrogel synthesis process is provided in Fig. 2. The main hydrogel composition studied in this investigation contained 1.5% w/v chitosan and 0.5% w/v genipin (Table 1). This is aligned with previous publications in which 1.5% w/v chitosan is commonly crosslinked with genipin concentrations ranging from 0.1–2% w/v.[32–39] High concentrations of chitosan are challenging to work with due to its solubility limitations and increased viscosity of solutions. Genipin concentrations less than 0.1% w/v are not recommended as resultant hydrogels are soluble in neutral and acidic conditions.[40] 0.5% w/v genipin was therefore used as it minimises potential cytotoxicity, while gels produced are stable and easy to handle. Concentration of constituents and NH_2 group calculations are provided in Table S1 (ESI†).

2.2.2 Hydrogel films. Chitosan and genipin solutions were prepared as described above, combined as defined in Table 1, and transferred to a Vision Plate™ 24 microplate. Following, the plate was sealed with a plastic cover and hydrogel films were formed in a UV-VIS spectrophotometer (BMG LABTECH, FLUOstar Omega Microplate Reader) at 37 °C for 24 hours.

2.3 Fluorescence studies

A UV-VIS spectrophotometer (BMG LABTECH, FLUOstar Omega Microplate Reader) was used to measure the fluorescence intensity (FI) of samples. Products formed by the reaction of genipin with primary amine groups are known to fluoresce in the 380 to 700 nm wavelength region.[41] In previous work, the crosslinking reaction of chitosan–genipin hydrogels was successfully followed using 550 nm and 650 nm for the excitation and emission wavelengths, respectively.[42] The same wavelengths were used in this study. The spectrophotometer was connected to a laptop with BMG LABTECH's Omega software. A bottom-up measurement was used to avoid measurement errors associated with condensation on the plastic cover. Well scans were used to allow the uniformity of fluorescence to be analysed. Within each well (diameter = 14.50 ± 0.10 mm), a matrix of 10 × 10 data points was scanned across 13 mm (scan area = 132.7^2), with 100 flashes per scan point and 0.2 s settling time. For each well, the average value of all scan points was used to plot FI against time.

2.4 Monitoring gelation

A preliminary study was conducted to determine when the crosslinking reaction between chitosan and genipin terminates. 500 μl of chitosan–genipin solution containing 1.5% w/v chitosan and either 0.5% v/v or 1% w/v genipin in a 5 : 1 volume ratio was added to wells and gelation was followed *in situ* by measuring FI every hour over 24 hours at 37 °C.

2.5 Lysozyme degradation

Chitosan–genipin hydrogels were degraded with lysozyme/PBS solution. The concentration of lysozyme in human tissues ranges from approximately 1.5 μg ml^{-1} to concentrations exceeding 1 mg ml^{-1}, depending on the tissue and infection status.[17,43–45] In previous gravimetric lysozyme degradation studies using 1.5 μg ml^{-1} lysozyme, no significant mass loss in chitosan–genipin hydrogels was observed after 28 days.[36,46] To accelerate degradation of hydrogel films and allow the study to be completed in a reasonable time, the lysozyme concentration was increased to 0.5 mg ml^{-1}. This concentration was previously reported as viable for accelerated degradation studies of chitosan–genipin hydrogels, with complete degradation occurring within approximately 14 days.[34] In experiments for disk degradation studies, the concentration was further increased to 6 mg ml^{-1} to enhance the degradation process and speed the experimentation (Supplementary Methods 1 and Fig. S3, ESI†). Hydrogel films were degraded *in situ*, and hydrogel disks were held in beakers containing lysozyme/PBS solution using 70 μm cell strainers.

Table 1 Hydrogel compositions and forms

Sample name	Geometry	Volume of 1.5% w/v chitosan solution (ml)	Volume of genipin solution (ml)	Concentration of genipin solution (% w/v)	Volume of chitosan–genipin solution containing 6 ml chitosan solution and 1.2 ml genipin solution (μl)	Volume ratio of chitosan to genipin
Vial 0.5	Disk[a]	1	0.2	0.5		5 : 1
Vial 1	Disk[a]	1	0.2	1		5 : 1
Well 0.5	Film[b]			0.5	500	5 : 1
Well 1	Film[b]			1	500	5 : 1

[a] Disks formed in cylindrical polyethylene vials (5 ml volume, 15 mm diameter) and used for FTIR and particle size analysis. [b] Films formed in the wells of Vision Plate™ 24 microplates and used for fluorescence studies and FTIR.

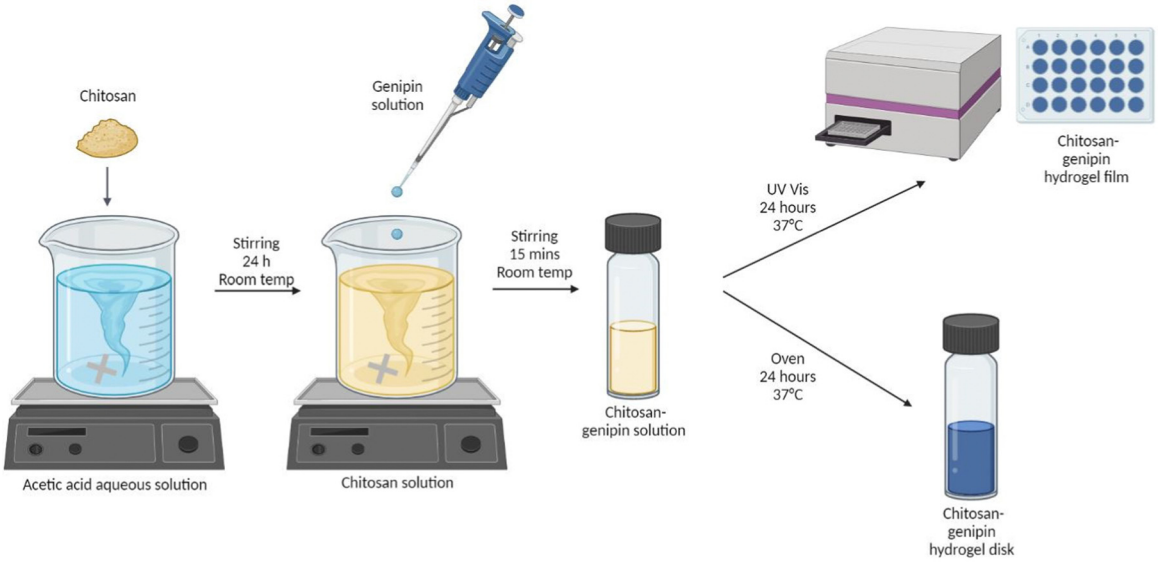

Fig. 2 Synthesis of chitosan–genipin hydrogel disks (created with BioRender).

2.5.1 Fluorescence degradation study of hydrogel films. Chitosan–genipin hydrogel films were formed for 24 hours in the wells of a Vision Plate™ 24 microplate (Section 2.2.2). At 24 hours, films were washed with deionised water before addition of 1 ml PBS solution containing 0.5 mg ml^{-1} of lysozyme. At scheduled times, the supernatants were aspirated, and FI of both hydrogels and supernatants was measured separately. The solutions were refreshed immediately after supernatant removal. The supernatants were stored in sealed vials, and FI was measured at future timepoints to test if FI changed over time. Both hydrogel films and supernatants were sealed and stored at 37 °C to resemble physiological conditions. The control hydrogel films were tested under the same conditions but were treated with PBS solution without lysozyme. The FI of additional controls was also measured. Control conditions included chitosan and genipin solutions alone, plus PBS and PBS/lysozyme solutions, in addition to PBS and lysozyme/PBS solutions alone.

2.6 Scanning electron microscopy

Scanning electron images were obtained using a Jeol JSM-5600LV scanning electron microscope (SEM) to determine the pore sizes of 1% w/v genipin hydrogels before and after immersion in PBS. Hydrogel disks were freeze dried prior to imaging by rapidly freezing samples in liquid nitrogen, followed by vacuum-drying in a Labconco freeze-dryer with the condenser set at −55 °C for 48 hours. Dried samples were mounted on an aluminium stub by means of a double side carbon sticky tape and sputtered with a 10 nm layer of Au in a Bio-Rad SC-500 Sputter Coater. The surface and internal microstructure of hydrogel disks were investigated at 20 kV acceleration voltage with a spot size of 24 and a working distance of 20 mm. The process of freeze drying can cause freezing stresses which may to some extent shrink and collapse outer surfaces of hydrogels,[32] therefore cross-sectional area is considered a better representative of native structure. ImageJ software was hence used to measure pore diameter using SEM images of horizontal cross sections.

2.7 Fourier transform infrared spectroscopy

Fourier-transform infrared (FTIR) spectroscopy was conducted to elucidate the chemical changes upon crosslinking and degradation of chitosan–genipin hydrogel disks. The reactions were quenched using the freeze drying procedure outlined in Section 2.5. Use of freeze-dried samples in FTIR minimises the presence of overlapping of peaks due to water molecules. An Agilent Technologies Cary 630 FTIR spectrometer equipped with diamond attenuated total reflection (ATR) was used to obtain FTIR spectra for samples between 4000–650 cm^{-1} in transmittance mode. 32 background scans were taken before 64 sample scans.

2.8 Zetasizer

Particle size measurements of lysozyme degradation products were performed on a Zetasizer (Nano ZS, Malvern Instruments, UK) at 25 °C using dynamic light scattering. Each sample was measured in 5 runs to calculate the average particle diameter. Malvern Zetasizer Software was used for data evaluation.

2.9 Mastersizer 3000

Particle size of lysozyme degradation products was also measured with the Mastersizer 3000 (Malvern, UK), using the light scattering method. The Hydro EV wet dispersion unit was used to analyse the liquid suspension, using deionised water as the dispersant. Each sample was measured in 5 runs to calculate the average particle diameter. Malvern Mastersizer Software was used for data evaluation.

2.10 Statistical analyses

Statistical analyses were performed using GraphPad Prism software. The data are presented as means ± standard deviation

and were compared using the either the Student's *t*-test or ANOVA and Tukey *post hoc* tests at 95% confidence level. *P* values less than 0.05 were considered significant.

3 Results and discussion

3.1 Monitoring gelation

The crosslinking reaction between chitosan and genipin produces a fluorescent product.[4,7,14,47] Fluorescence can therefore be used to monitor the gelation progress of chitosan–genipin hydrogels. FI was measured from the moment all constituents were combined up to 24 hours, to allow the gelation process to be assessed (Sections 2.2 and 2.3). Fig. 3 shows that for both hydrogel compositions studied, the increase in FI is greatest at the start of the reaction, due to the rate of reaction being a function of the concentrations of genipin and amine groups. In particular, this reaction is dependent on the concentration of genipin, which is the limiting reactant (Table S1, ESI†), and in this batch-like reaction system falls over time, proportionally reducing the rate of the crosslinking process. The role genipin plays in the rate of crosslinking process is also confirmed with a positive correlation observed between genipin concentration and the rate of crosslinking (Fig. 3). Increasing the concentration of crosslinking agent should result in a higher degree of crosslinking, and therefore a higher FI. However, the maximum fluorescence for all hydrogels appeared to be approximately 4600 (AU). It is possible that the blue colour produced due to the crosslinking reaction reduced the penetration depth of the excitation light, leading to a plateau in FI.[48] In the hydrogels produced with 1% w/v genipin, once maximal fluorescence is reached at ~8 hours, FI gradually decreases. The decrease in FI is possibly due to collisional quenching during a diffusive encounter with amines and the complex formation by further polymerisation.[15] In contrast, maximal fluorescence is reached at ~14 hours in the 0.5% w/v genipin hydrogels, and plateaus from this point onwards. Overall, this preliminary study shows that the chitosan–genipin crosslinking reaction terminates before 24 hours, therefore 24 hours is a suitable time to start degradation studies.

3.2 Fluorescence degradation study of chitosan hydrogel films

The degradation of chitosan–genipin hydrogel films exposed to 0.5 mg ml^{-1} lysozyme/PBS was assessed using florescence studies (Section 2.4.1). As fluorescence is proportional to the degree of crosslinking, FI of both hydrogels and degradation solutions was measured over time to monitor degradation and to determine if lysozyme can degrade chitosan–genipin crosslinks. The FI of various controls was also measured (Fig. S4, ESI†). For most controls, a low FI of approximately 250 AU was detected. This background fluorescence is extremely low compared the FI of formed hydrogels (4600 AU). When genipin solution was mixed with lysozyme solution (Fig. S4F, ESI†), the FI followed a triphasic pattern. There was a rapid increase to ~1700 within 5 hours, followed by a gradual increase to ~4500 AU by around 4 days and a slow decrease after reaching maximum FI. This result was expected as lysozyme is a protein consisting of 129 amino acids, therefore genipin can react with the amino groups to generate a fluorescent product. However, for both hydrogel compositions, it was calculated that all genipin crosslinking sites would be saturated, meaning no further reaction with lysozyme should have occurred (Table S1, ESI†). Furthermore, the hydrogels were washed with deionised water prior to addition of relevant solutions, which should have removed any unreacted genipin if present. It can therefore be assumed that the fluorescence assessed in the study is due to the interaction between chitosan and genipin only.

Fig. 4C shows the lysozyme degradation of chitosan–genipin films formed with 0.5% w/v genipin follows a triphasic pattern. During the first few days after lysozyme exposure, there was no change in FI, indicating no degradation had occurred. On day 3, the FI slowly started to decrease and decreased exponentially from day 6 until the matrix was completely broken down, upon vial inspection, two days later. This initial 'induction period' may occur for a number of reasons. First, the crosslinked

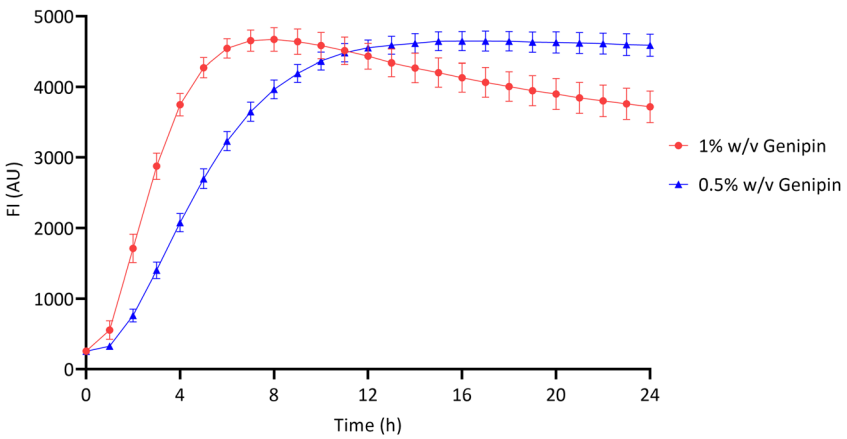

Fig. 3 Fluorescence intensity of chitosan–genipin hydrogels during their formation over 24 hours. Data are presented as the mean ± standard deviation where $n = 4$.

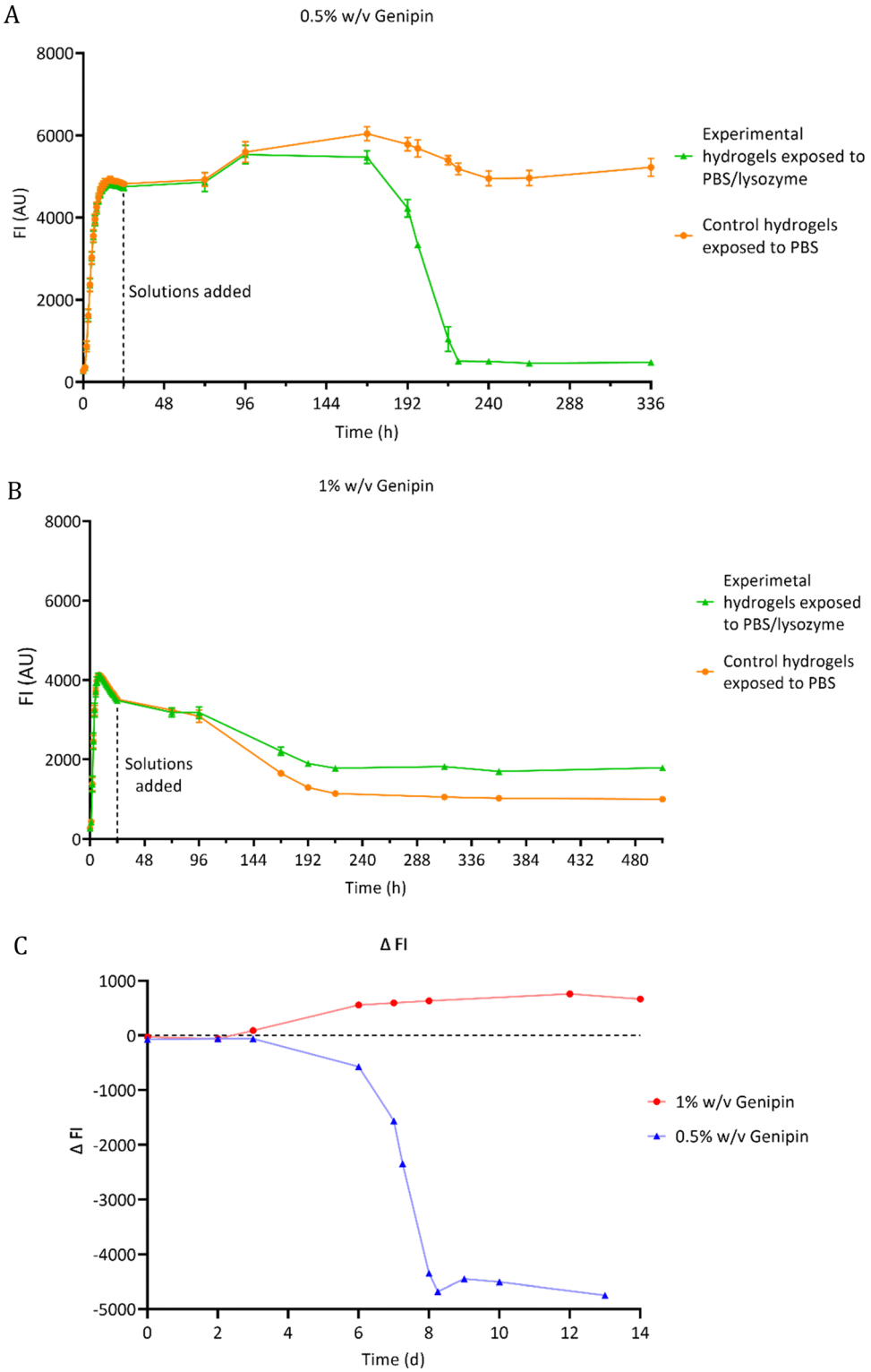

Fig. 4 FI of chitosan–genipin hydrogel films following lysozyme degradation. (A) Hydrogels formed with 0.5% w/v genipin; (B) hydrogels formed with 1% w/v genipin; (C) relative FI where ΔFI = FI measured in control sample is subtracted from FI measured in lysozyme-treated sample. Data are presented as the mean ± standard deviation where n = 3.

structure of the hydrogel likely limits the penetration of lysozyme into the hydrogel and subsequently impedes the formation of enzyme–substrate complexes. Further, as lysozyme only binds to the NAG units of chitosan,[26] and cleavage of the glycosidic bond occurs exclusively between subsites D and E,[49] it may take time for the enzyme–substrate complexes to form. We postulate

that once initial degradation occurs, it is easier for subsites D and E to engage with shorter acetylated oligosaccharides, resulting in an increased rate of hydrolysis. Well scans were performed in fluorescence studies to allow the gel structure to be analysed (Fig. S5, ESI†). Lysozyme degradation of hydrogel films contained in wells would be expected to occur downwards in a uniform manner. Interestingly, lysozyme degradation is initiated from one side of the gel and propagates outwards from this point, supporting the theory that lysozyme degradation is an autocatalytic reaction.

When the genipin concentration of hydrogels was increased to 1% w/v, the degradation kinetics markedly changed (Fig. 4B). Lysozyme treatment only reduced FI of these hydrogels by 49%, compared to 90% in the 0.5% w/v genipin hydrogels, indicating that substantially less degradation occurred (Fig. 4A and B). This is consistent with gravimetric degradation studies where no significant mass loss was observed in chitosan–genipin gels, albeit the lysozyme concentrations used were much lower.[36,50] The higher concentration of genipin in the 1% w/v genipin hydrogels likely increased the crosslinking density of the resultant scaffold, resulting in a tighter structure that impeded lysozyme penetration and subsequent degradation. Furthermore, gravimetric swelling studies showed that the 0.5% w/v genipin hydrogels swell slightly upon immersion into PBS solution (pH 7.4 ± 0.2), which may have expanded the hydrogel structure and assisted lysozyme infiltration (Supplementary Method 2 and Fig. S6, ESI†). In contrast, the 1% w/v genipin hydrogels did not exhibit any initial increase in volume and had a higher degree of contraction. When solution pH is above the dissociation constant of chitosan (6.5–6.7), chitosan's free amino groups are deprotonated, resulting in reduced electrostatic repulsion and contraction of the network.[32] Other studies report that increasing genipin concentration significantly decreases the swelling ratio of chitosan hydrogels immersed in PBS.[36,51] It is likely that 1% w/v genipin hydrogels contracted more due to enhanced crosslinked structure, resulting in closer proximity of chitosan amino groups, which exhibit deprotonation and hydrogel shrinking in PBS solution (7.4 ± 0.2). SEM images of 1% w/v genipin hydrogels were obtained to determine the effect of PBS on pore size (Fig. S7, ESI†). The average pore diameter of formed 1% w/v genipin hydrogels was 68.6 μm ± 18.0, which significantly decreased to 20.8 μm ± 9.7 ($p < 0.0001$) after immersion in PBS for 1 week. It is possible that enhanced hydrogel contraction and further pore size reduction occurred in 1% w/v genipin hydrogels, obstructing lysozyme entry and reducing interaction with chitosan. Interestingly, control hydrogels formed with 1% w/v genipin, exposed to PBS alone, had lower FI measurements compared to the experimental hydrogels treated with PBS/lysozyme (Fig. 4B). This result was unexpected, as lysozyme should degrade the hydrogel and reduce FI. It was visually noted that the control gels shrunk more than the experimental gels, explaining the decrease in FI. As shown in Fig. S6 (ESI†), hydrogels crosslinked with 1% w/v genipin shrunk more than those formed with 0.5% w/v genipin. It is possible that when lysosome (and PBS) was added to the 1% w/v genipin hydrogel, it degraded the material to some extent, reducing the crosslinking degree and weakening the structure, which resulted in less shrinking compared to control hydrogel exposed to PBS alone.

3.3 Fluorescence measurements of supernatants

Hydrogel films were formed wells (Section 2.2) and lysozyme solution was added on top of the gels. At scheduled times, supernatants were aspirated from the wells and FI of the liquid was measured. Supernatant from hydrogels exposed to PBS alone and fresh lysozyme/PBS solution served as controls. Fig. 5 shows that throughout the experiment, the FI of supernatants of hydrogels exposed to lysozyme/PBS solution was significantly higher than both controls. This suggests that the chitosan–genipin crosslinks were present in the supernatant. The FI of experimental supernatant was highest on day 6 post lysozyme addition, which correlates with the sudden decrease in FI of

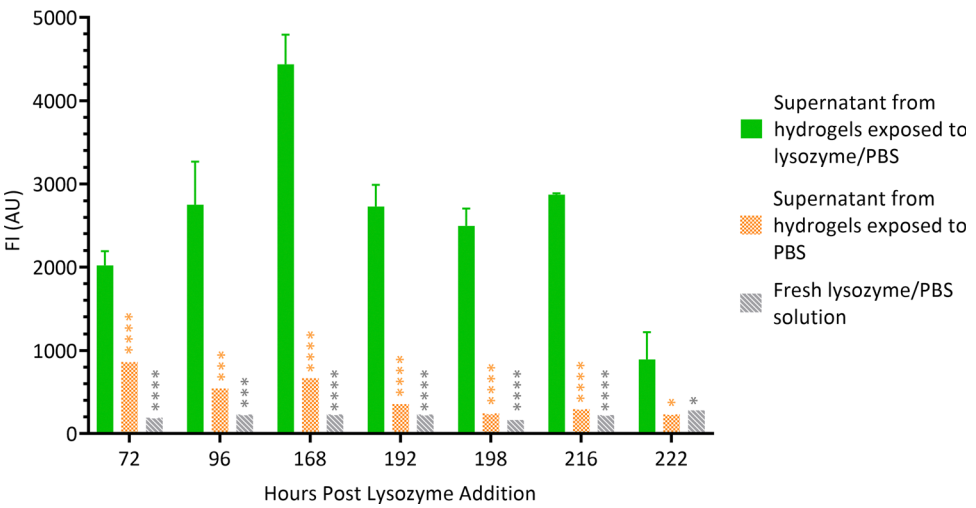

Fig. 5 FI of lysozyme degradation solutions at various time points. Data are presented as the mean ± standard deviation where $n = 3$, *$P < 0.05$, ***$P < 0.001$ and ****$P < 0.0001$.

the hydrogel. The supernatants were stored in sealed vials and FI was monitored at future timepoints. The FI of supernatants remained relatively stable over time (Fig. S8, ESI†). This suggests that the lysozyme degradation products do not undergo further degradation by the enzyme.

3.4 Monitoring crosslinks with FTIR

FTIR spectroscopy was conducted to determine the mechanism by which lysozyme degrades crosslinks in chitosan–genipin hydrogel disks (Fig. 6A). Table 2 presents a summary of the band assignments of all investigated FTIR spectra. First, FTIR spectra were obtained for chitosan powder, genipin solution and freeze-dried chitosan–genipin hydrogel disks that had undergone gelation for 24 hours to identify the chemical changes induced by crosslinking. A wide band at 3600–3000 cm^{-1} is present in the chitosan and hydrogel spectra, which is attributed to overlapping O–H and N–H stretching vibrations.[52] All samples have a band at approximately 2900 cm^{-1} corresponding to C–H stretching of the pyranose ring,[53,54] in addition to a peak at 2100 cm^{-1} which originates from C–C of the diamond used in attenuated total reflectance measurement.[42] Genipin's characteristic transmission peaks are observed at 1679 cm^{-1} and 1618 cm^{-1}, which represent C=C stretching of the carboxymethyl group and C=C aromatic stretching, respectively.[42,55]

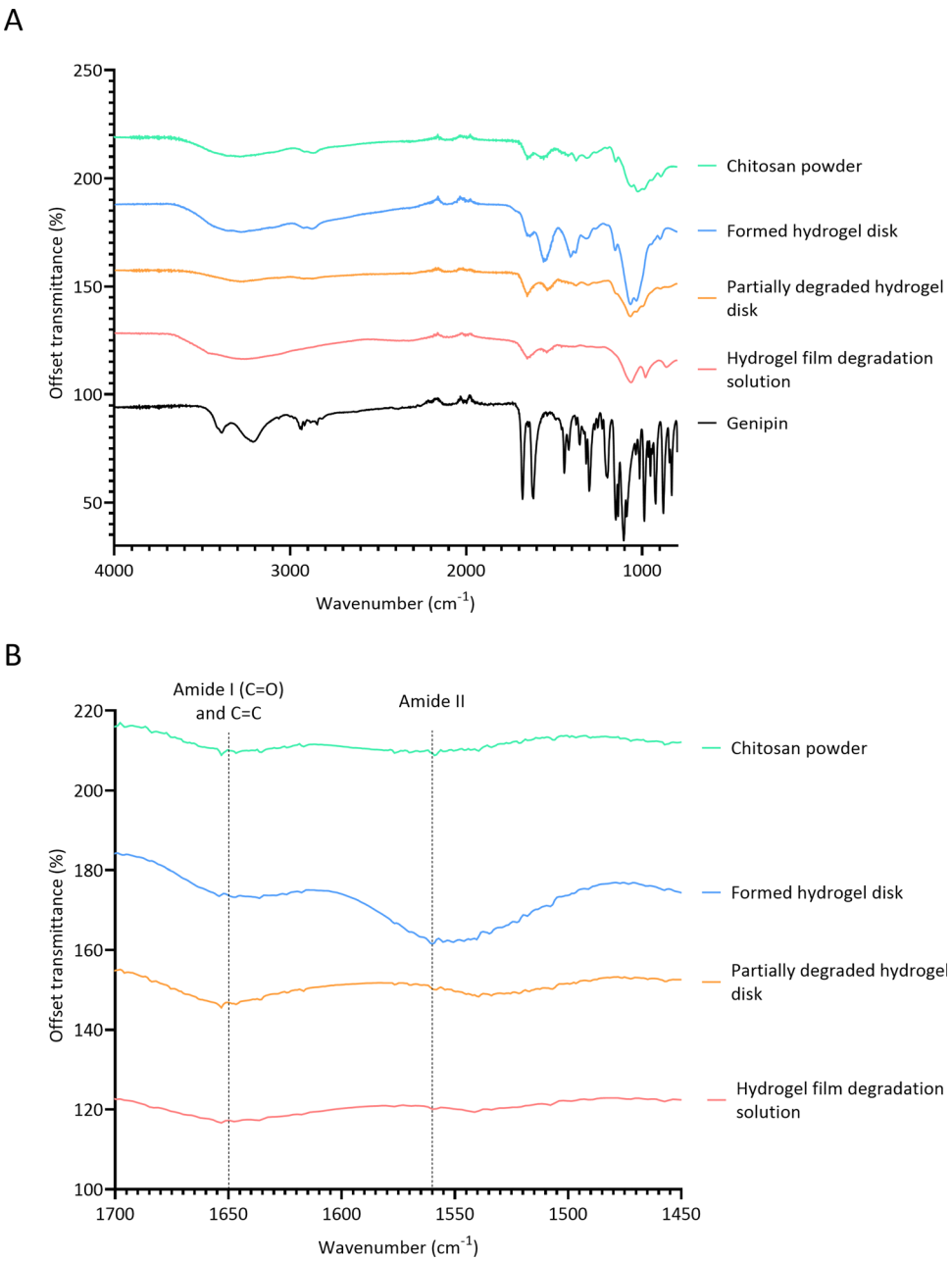

Fig. 6 FTIR spectra. (A) Full FITR spectra of individual hydrogel constituents, formed hydrogel and degraded hydrogel samples; (B) FTIR spectra focusing on amide I, C=C and amide II bands.

Table 2 FTIR characteristics bands for individual hydrogel constituents, formed hydrogel disk and degraded hydrogel samples assigned using the literature

Band assignment	Wavenumber (cm^{-1})				
	Chitosan powder	Genipin	Formed hydrogel disk	Partially degraded hydrogel disk	Hydrogel film degradation solution
Overlap of O–H and N–H stretching (primary amine)	3600–3000	3390 (O–H only)	3600–3000	3600–3000	3600–3000
C═C–H stretching		3211			
C–H stretching (pyranose ring)	2864	2935	2869	2873	
C═O stretching (amide I)	1647		1636	1647	1653
C═C stretching (cyclic alkene)	1647	1679	1636	1653	1653
C–C stretch from cycloolefin		1618			
N–H bending (amide II)	1559		1560	1539	1541
CH_2 bending (CH_2OH group)	1410	1442	1404	1437	1541
CH_3 bending (*n*-acetyl group)	1375		1378	1374	
C–N stretching (amide III)	1312		1315	1307	
C–O–C stretching	1149		1153		
C–O stretching	1059, 1023, 991		1065, 1032	1065, 1032	1062, 977
C–N stretching	1059, 1023, 991		1065, 1032	1065, 1032	1062, 977
C–O–C asymmetric stretching of methyl ester		1300, 1104			
C–H bending out of plane	894	987	898	893	861

Two distinctive peaks are observed in the chitosan spectrum at 1647 cm^{-1} and 1559 cm^{-1}. The former represents C═O stretching of the secondary amide (amide I band) present in the acetylated units of chitosan, and the latter is due to N–H bending in the secondary amide (amide band II). These peaks are also observed in the hydrogel spectrum; however, the wavenumbers are slightly shifted. Following gelation, both the amide I and amide II bands increase in intensity (Fig. 6B and Table S2, ESI†). This shows that the amino groups of the chitosan have reacted with carboxymethyl groups of genipin to form secondary amides (Fig. 1).[32,52] Overlap between the C═O stretching band in secondary amides with the C═C stretching of the olefin ring in genipin causes the amide I band to become slightly broader in curve.[50,56] Fig. 6A shows that gelation causes the peak at approximately 1400 cm^{-1} to increase in intensity. Some articles report that this band is due to CH_2 bending deformations in the CH_2OH group,[57,58] with others assigning this band to O–H bending.[34,59,60] Both functional groups have transmittance values within this region, and both types of bonds would be expected to increase in hydrogels. The band at 1375 cm^{-1} is assigned to CH_3 bending of the acetylated units of chitosan.[53,57] In the hydrogel spectrum, this band is also due to the aromatic C–N stretch in the newly formed tertiary amine,[61] explaining the increase in intensity. The band at 1312 cm^{-1} corresponds to C–N stretching in secondary amides (amide III), present in both chitosan powder and hydrogel spectra.[57,58,62] The band intensity slightly increases in the hydrogel spectra by virtue of the crosslinking reaction, generating additional secondary amides. The transmission band at 1149 cm^{-1} in the spectra of the chitosan powder and formed hydrogel is attributed to asymmetric stretching of the C–O–C bridge from the glycosidic bond.[57,63] Transmission bands observed is the chitosan spectrum at 1059 cm^{-1} and 1023 cm^{-1} are attributed to aliphatic C–N stretching and C–O stretching vibrations in alcohols.[52,60] In the hydrogel spectrum, the band corresponding to aliphatic C–N stretching increases in intensity, likely due to the newly formed tertiary amine.[50] Butler *et al.* reported that the formation of C–N bonds at the expense of C–O bonds occurs during the formation of the heterocyclic genipin–chitosan compound.[14]

FTIR was then performed on two degradation samples to determine if lysozyme effects the chemical changes induced by crosslinking. Samples investigated included partially degraded hydrogel disks exposed to 0.5 mg ml^{-1} lysozyme/PBS solution for 24 days and the product remaining from the evaporated degradation solution of hydrogel films. After the addition of lysozyme, the C–O–C bridge transmission band at 1149 cm^{-1} is no longer observed in the FTIR spectrum. This shows that lysozyme hydrolysed the β-(1,4) linkages between the D-glucosamine and *N*-acetyl-D-glucosamine units in chitosan (Fig. S2, ESI†). Interestingly, the band corresponding to alcoholic C–O stretching remains relatively high in the degraded hydrogel. This further confirms that lysozyme hydrolysis has occurred, whereby the C–O–C bridge is replaced with a hydroxyl group. Fig. 6A shows that the FTIR spectrum of the partially degraded hydrogel is extremely comparable to the chitosan powder spectrum, suggesting that lysozyme degrades crosslinks and reverts the hydrogel closer to its primitive structure. The peaks observed at 1560 cm^{-1} and 1315 cm^{-1} the hydrogels, corresponding to amide band II and amide band III, respectively, markedly reduce in intensity in the degraded hydrogel. This indicates that there is a reduction in secondary amides, suggesting that one of the bifunctional crosslinks between chitosan–genipin structure is broken. In both degradation samples, the intensity of the band at 1647 cm^{-1} remains relatively high. The peak height and peak height ratios between amide I and amide II bands were obtained for all samples (Table S2, ESI†). In the chitosan powder, the ratio is almost equal. As crosslinking proceeds, the proportion of amide II bands increases (1 : 1.68). However, post lysozyme degradation, the ratio of

amide I to amide II bands increases (~1 : 0.80). Interestingly, in degraded samples, the amide II peak height almost returns to baseline, whereas the amide I band decreases slightly but remains higher than native chitosan. As there is overlap between C=O stretching and C=C stretching, these results suggest that lysozyme breaks the amide bonds, whilst the C=C bonds in cyclic alkenes are unaffected. Furthermore, in the degradation samples, the band corresponding to aliphatic C–N stretching remains high relative to the adjacent band assigned to C–O stretching. Overall, these results suggest that lysozyme degrades the secondary amide linkage, whilst the tertiary aromatic amine linkage remains intact. It is therefore possible that the highly conjugated heterocyclic genipin derivatives in chitosan–genipin hydrogels are still present post lysozyme treatment, explaining why the degradation solution exhibited fluorescent properties, which remained stable over an extended period of time (Fig. S8, ESI†).

3.5 Particle size of lysozyme degradation products

Chitosan–genipin disks were degraded with lysozyme, and degradation solution (Section 2.4) was analysed with the Zetasizer to measure particle size (Section 2.7). The unfiltered degradation solution showed three populations of fragments, with particle sizes ranging from 78.8 nm to 5559.6 nm (Fig. 7A). As it took approximately 12 days for the hydrogel disks to degrade (visual inspection), it is likely that over time the degradation particles accumulated at the bottom of the vessel, promoting the formation of weak inter-particle forces, such as van der Waals or electrostatic, resulting in agglomeration of particles. In a previous study, SEM images showed that glutaraldehyde-crosslinked chitosan nanoparticles agglomerate after incubation with lysozyme solution.[54] The Mastersizer 3000 was used to test for agglomeration through detection of larger particles (Section 2.8). Disk degradation studies were conducted using 70 μm cell strainers (Section 2.4), therefore initial degradation fragments were <70 μm. Mastersizer 3000 results showed that the mean particle size was 218.40 μm ± 17.8, evidencing that particle agglomeration took place. A 0.22 μm cell strainer was used to further filter the degradation solution to test if any smaller particles were present. The filtered degradation solution displayed a bimodal size distribution with average sizes of 5.0 nm ± 0.5 and 357.0 nm ± 10.4 (Fig. 7B). It is likely that these smaller particles were not detected in the unfiltered solution as the larger particles obscured them from the incident laser beam.

The kidneys are the primary excretory organ of the body. The 3 steps of renal elimination are: glomerular filtration, resorption and secretion. The glomerular filtration barrier is a three-layer specialised blood filtration interface that selectively filters molecules based on size and electrical charge. The slit diaphragm is the final barrier preventing passage of macromolecules into the urinary filtrate. Foot processes of the podocytes form small slits of 5 nm and are surrounded by anionic glycocalyx.[64–67] The cationic nature of chitosan should, therefore, aid the excretion of chitosan degradation products by the kidneys. The two-pore theory of glomerular filtration states that the transcapillary passage of proteins across the glomerular membrane occurs *via* two distinct porous pathways; passage of small solutes and water mainly occurs through small pores whereas larger macromolecules pass through larger pores, referred to as 'shunt pathways'.[68,69] Experimental studies using dextrans as tracer macromolecules show that the mean radius of small pores in the glomerular capillary are approximately 5 nm, in both humans and rats.[70,71] Choi *et al.* employed fluorescent quantum dots to precisely determine the hydrodynamic radius that permits clearance of nanoparticles in rats. A hydrodynamic radius of <5.5 nm resulted in rapid and efficient urinary excretion, however, a hydrodynamic radius of over 15 nm prevented renal excretion.[72] Tencer *et al.* assessed the glomerular transport of endogenous proteins with varying radii and found that large pores with a radius of 11–11.5 nm account for the clearance of large proteins into the primary urine.[73] However, in physiological conditions, the shunt pathways are only permeated by approximately 1×10^{-4}% of filtrate.[74] It is generally accepted that proteins of the size of immunoglobulin (molecular radius of 5.5 nm) are almost completely restricted from glomerular filtration, as their radius exceeds the size of the small pores, and the contribution of shunt pores in quantitatively irrelevant.[74] In accordance with these findings, it can be assumed that particles with a diameter

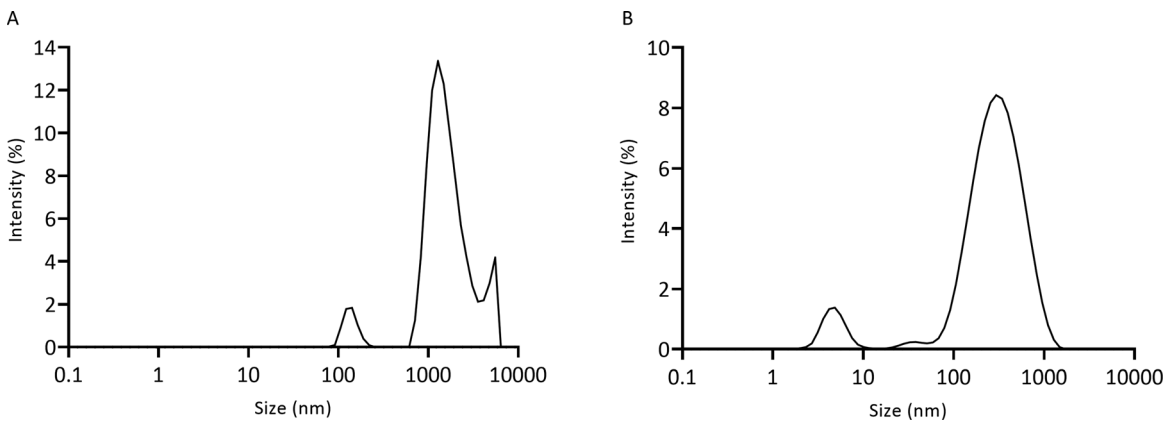

Fig. 7 Particle size of lysozyme-degraded chitosan–genipin hydrogel disks measured by the Zetasizer. (A) Unfiltered solution; (B) filtered solution.

of <5.5 nm can be excreted by the small pores of the kidneys. A small population of filtered chitosan–genipin hydrogel degradation products were below this threshold, with the smallest detected particle size being 1.7 nm, suggesting that chitosan–genipin hydrogels can potentially be eliminated by the renal system *in vivo*. Furthermore, breakage of glycosidic bonds in chitosan results in the formation of oligosaccharides and monosaccharides that can subsequently be incorporated into glycosaminoglycans and glycoproteins, or be excreted.[75] The length of a monomer unit of chitosan has been reported as 0.52 nm.[76,77] Studies in rats show that $>80\%$ of administered chitosan is excreted in urine within approximately 11 day.[78,79] When glucosamine or *N*-acetylglucosamine are intravenously administrated in humans, both aminomonosaccharides are readily eliminated from the blood, with over 50% excreted in the urine.[80] As chitosan monosaccharide units are smaller than the degradation particles of chitosan–genipin hydrogels, this suggests that the hydrogels are not completely degraded by lysozyme, with some crosslinks remaining intact.

An alternative route of elimination for nanoparticles exceeding 5.5 nm is the liver. The pore size of fenestrae in liver sinusoidal endothelial cells are 100–200 nm. Therefore, particles smaller than this size limit can pass through fenestrations, be processed by hepatocytes, and ultimately be removed from the body *via* faeces.[64] In this study, particles below this size limit were detected by the Zetasizer, for example, 33% of unfiltered particles were <200 nm. This suggests that in the case of incomplete degradation or agglomeration of smaller particles, biliary excretion of chitosan–genipin hydrogels may occur *in vivo*. When nanomaterials bypass the renal and biliary excretory systems of the body, they accumulate in the reticuloendothelial system, namely in liver and spleen macrophages.[64] Sadauskas and colleagues intravenously and intraperitoneally administered gold nanoparticles to mice and found that they primarily accumulated in Kupffer cells in the liver.[81] Kupffer cells are liver-resident macrophages that internalize nanoparticles through various receptors including scavenger, toll-like, mannose, and Fc receptors. Phagocytosis is the cellular process of ingesting and eliminating particles including microorganisms, foreign substances, and apoptotic cells.[82,83] It involves several key steps: (i) detection of the particle to be ingested, (ii) activation of the internalization process, (iii) phagosome formation, and (iv) maturation of the phagosome to transform it into a phagolysosome. Phagosomes are highly acidic, contain many hydrolytic enzymes and generate reactive oxygen species, that enable degradation and digestion of internalised particles.[82,84] Studies have reported that particles >10 μm are capable of being phagocytosed, with the optimal diameter being 2–3 μm.[85–90] If the particle size is between 10–100 μm, macrophages fuse together to form foreign body giant cells capable of engulfing these larger particles. When particles exceed 100 μm, bulk digestion is carried out *via* extracellular degradation.[91] However, regardless of the size, non-degradable substances will be retained in the body indefinitely. If degradation fails, foreign body giant cells will recruit fibroblasts to form a capsule around the material, creating a physical barrier to isolate it from the host.[92]

4 Conclusions

This study demonstrated that the crosslinking reaction between chitosan and genipin produces highly conjugated heterocyclic structures, resulting in the formation of fluorescent hydrogels. Fluorescence degradation studies showed that the supernatant of degraded hydrogels significantly fluoresced, suggesting that although the hydrogel structure was broken down, fluorescent relevant chitosan–genipin crosslinks remained intact. FTIR was employed to elucidate the chemical changes induced by crosslinking and lysozyme degradation. Upon gelation there was an increase in several secondary amide bonds, indicating the amino groups of chitosan reacted with the carboxymethyl groups of genipin to form secondary amides. The intensity of these bonds reduced after lysozyme treatment, showing secondary amide crosslinks were broken. Overlap exists between C═O stretching in secondary amides with C═C stretching of the olefin ring in genipin, collectively referred to in this study as amide I band. In lysozyme-degraded hydrogels, the intensity of amide I was higher compared to native chitosan. This result suggests that C═C bonds are unaffected by lysozyme. Our findings indicate that in chitosan–genipin hydrogels, lysozyme degrades the secondary amide linkage, whilst the tertiary aromatic amine linkage remains intact. It is, therefore, possible that the highly conjugated heterocyclic genipin structures are present in hydrogel degradation products, accounting for the detected fluorescence in the supernatant. Analysis of hydrogel/lysozyme solutions following degradation of hydrogels using Zetasizer measurements showed that a small population of degradation particles were <5.5 nm, indicating feasibility of renal elimination *in vivo*. Furthermore, clusters of larger particles are shown to be likely formed *via* agglomeration. Results show promise and potential for the use of chitosan–genipin hydrogels *in vivo*, however, *in vivo* studies are ultimately required to establish their biodistribution and biodegradability, in which the intrinsic fluorescence of these hydrogels could be used as a detection tool. Additional *in vitro* co-culture studies with lysozyme-degraded chitosan–genipin hydrogels and macrophages should be conducted to determine if these particles can be phagocytosed and digested by the phagolysosome.

Author contributions

All authors contributed to the conceptualization of the project and review and editing of the manuscript. SR planned and performed the experiments and wrote the original draft. KN was involved in methodology design, project supervision and manuscript writing.

Conflicts of interest

There are no conflicts of interest to declare.

Acknowledgements

This work was supported by UK Engineering and Physical Sciences Research Council Doctoral Training Partnership

(EPSRC DTP) scholarship (project reference 2442338) and *Versus* Arthritis (grant number 22072). SEM work was conducted by the Electron Microscopy and Analysis Unit within the SAgE Analytical Facility at Newcastle University. All data created during this research are openly available at **https://doi.org/10.25405/data.ncl.c.6161178.v1**.

References

1 E. Caló and V. V. Khutoryanskiy, Biomedical applications of hydrogels: A review of patents and commercial products, *Eur. Polym. J.*, 2015, **65**, 252–267.
2 E. M. Ahmed, Hydrogel: Preparation, characterization, and applications: A review, *J. Adv. Res.*, 2015, **6**(2), 105–121.
3 Q. Chai, Y. Jiao and X. Yu, Hydrogels for Biomedical Applications: Their Characteristics and the Mechanisms behind Them, *Prog. Colloid Polym. Sci.*, 2017, **3**(1), 6.
4 K. Novakovic, S. Matcham and A. Scott, *Hydrogels*, Gels Horizons: From Science to Smart Materials, 2018, pp. 1–28.
5 M. Rinaudo, Chitin and chitosan: Properties and applications, *Prog. Polym. Sci.*, 2006, **31**(7), 603–632.
6 H. M. Ibrahim and E. M. R. El-Zairy, *Concepts, Compounds and the Alternatives of Antibacterials*, 2015.
7 R. A. A. Muzzarelli, M. E. Mehtedi, C. Bottegoni, A. Aquili and A. Gigante, Genipin-Crosslinked Chitosan Gels and Scaffolds for Tissue Engineering and Regeneration of Cartilage and Bone, *Mar. Drugs*, 2015, **13**(12), 7314–7338.
8 J. Nilsen-Nygaard, S. Strand, K. Vårum, K. Draget and C. Nordgård, Chitosan: Gels and Interfacial Properties, *Polymers*, 2015, **7**(3), 552–579.
9 V. Zargar, M. Asghari and A. Dashti, A Review on Chitin and Chitosan Polymers: Structure, Chemistry, Solubility, Derivatives, and Applications, *ChemBioEng Rev.*, 2015, **2**(3), 204–226.
10 R. Harris, E. Lecumberri and A. Heras, Chitosan–genipin microspheres for the controlled release of drugs: clarithromycin, tramadol and heparin, *Mar. Drugs*, 2010, **8**(6), 1750–1762.
11 K. Varaprasad, G. M. Raghavendra, T. Jayaramudu, M. M. Yallapu and R. Sadiku, A mini review on hydrogels classification and recent developments in miscellaneous applications, *Mater. Sci. Eng., C*, 2017, **79**, 958–971.
12 H. W. Sung, R. N. Huang, L. L. H. Huang and C. C. Tsai, In vitro evaluation of cytotoxicity of a naturally occurring cross-linking reagent for biological tissue fixation, *J. Biomater. Sci., Polym. Ed.*, 1999, **10**(1), 63–78.
13 N. L. Delgadillo-Armendariz, N. A. Rangel-Vazquez, E. A. Marquez-Brazon and B. R. D. Gascue, Interactions of chitosan/genipin hydrogels during drug delivery: a qspr approach, *Quim. Nova*, 2014, **37**(9), 1503–1509.
14 M. F. Butler, Y. F. Ng and P. D. A. Pudney, Mechanism and kinetics of the crosslinking reaction between biopolymers containing primary amine groups and genipin, *J. Polym. Sci., Part A: Polym. Chem.*, 2003, **41**(24), 3941–3953.
15 H. Chen, W. Ouyang, B. Lawuyi, C. Martoni and S. Prakash, Reaction of chitosan with genipin and its fluorogenic attributes for potential microcapsule membrane characterization, *J. Biomed. Mater. Res., Part A*, 2005, **75A**(4), 917–927.
16 C. Wang, T. T. Lau, W. L. Loh, K. Su and D. A. Wang, Cytocompatibility study of a natural biomaterial cross-linker–Genipin with therapeutic model cells, *J. Biomed. Mater. Res., Part B*, 2011, **97**(1), 58–65.
17 J. Brouwer, T. Leeuwen-Herberts and M. O. V. Ruit, Determination of lysozyme in serum, urine, cerebrospinal fluid and feces by enzyme immunoassay, *Clin. Chim. Acta*, 1984, **142**(1), 21–30.
18 M. Klockars and S. Reitamo, Tissue distribution of lysozyme in man, *J. Histochem. Cytochem.*, 1975, **23**(12), 932–940.
19 D. Y. Mason and C. R. Taylor, The distribution of muramidase (lysozyme) in human tissues, *J. Clin. Pathol.*, 1975, **28**(2), 124.
20 L. Jiang, Y. Li, L. Wang, J. Guo, W. Liu and G. Meng, *et al.*, Recent Insights Into the Prognostic and Therapeutic Applications of Lysozymes, *Front. Pharmacol.*, 2021, **12**, 767642.
21 J. D. Funkhouser and N. N. Aronson, Chitinase family GH18: evolutionary insights from the genomic history of a diverse protein family, *BMC Evol. Biol.*, 2007, **7**(1), 96.
22 R. T. Ellison and T. J. Giehl, Killing of Gram-negative bacteria by lactoferrin and lysozyme, *J. Clin. Invest.*, 1991, **88**(4), 1080–1091.
23 W. T. Oliver and J. E. Wells, Lysozyme as an alternative to growth promoting antibiotics in swine production, *J. Anim. Sci. Biotechnol.*, 2015, **6**(1), 35.
24 N. C. J. Strynadka and M. N. G. James, Lysozyme revisited: Crystallographic evidence for distortion of an N-acetylmuramic acid residue bound in site D, *J. Mol. Biol.*, 1991, **220**(2), 401–424.
25 D. E. Koshland, Stereochemistry and the mechanism of enzymatic reactions, *Biol. Rev.*, 1953, **28**(4), 416–436.
26 A. Kristiansen, K. M. Varum and H. Grasdalen, The interactions between highly de-N-acetylated chitosans and lysozyme from chicken egg white studied by 1H-NMR spectroscopy, *Eur. J. Biochem.*, 1998, **251**(1–2), 335–342.
27 L. R. Berger and R. S. Weiser, The β-glucosaminidase activity of egg-white lysozyme, *Biochim. Biophys. Acta*, 1957, **26**(3), 517–521.
28 R. J. Nordtveit, K. M. Vårum and O. Smidsrød, Degradation of fully water-soluble, partially N-acetylated chitosans with lysozyme, *Carbohyd. Polym.*, 1994, **23**(4), 253–260.
29 W. W. Thein-Han and Y. Kitiyanant, Chitosan scaffolds for in vitro buffalo embryonic stem-like cell culture: An approach to tissue engineering, *J. Biomed. Mater. Res., Part B*, 2007, **80B**(1), 92–101.
30 D. Ren, H. Yi, W. Wang and X. Ma, The enzymatic degradation and swelling properties of chitosan matrices with different degrees of N-acetylation, *Carbohyd. Res.*, 2005, **340**(15), 2403–2410.
31 N. Islam, I. Dmour and M. O. Taha, Degradability of chitosan micro/nanoparticles for pulmonary drug delivery, *Heliyon*, 2019, **5**(5), e01684.
32 N. T. N. Vo, L. Huang, H. Lemos, A. Mellor and K. Novakovic, Poly(ethylene glycol)-interpenetrated genipin-crosslinked

chitosan hydrogels: Structure, pH responsiveness, gelation kinetics, and rheology, *J. Appl. Polym. Sci.*, 2020, **137**(41), 49259.

33 S. Matcham and K. Novakovic, Fluorescence Imaging in Genipin Crosslinked Chitosan–Poly(vinyl pyrrolidone) Hydrogels, *Polymers*, 2016, **8**(11), 385.

34 N. T. N. Vo, L. Huang, H. Lemos, A. L. Mellor and K. Novakovic, Genipin-crosslinked chitosan hydrogels: Preliminary evaluation of the in vitro biocompatibility and biodegradation, *J. Appl. Polym. Sci.*, 2021, **138**(34), 50848.

35 A. A. Aldana, A. González, M. C. Strumia and M. Martinelli, Preparation and characterization of chitosan/genipin/poly(N-vinyl-2-pyrrolidone) films for controlled release drugs, *Mater. Chem. Phys.*, 2012, **134**(1), 317–324.

36 L. Bi, Z. Cao, Y. Hu, Y. Song, L. Yu and B. Yang, *et al.*, Effects of different cross-linking conditions on the properties of genipin-cross-linked chitosan/collagen scaffolds for cartilage tissue engineering, *J. Mater. Sci. Mater. Med.*, 2010, **22**(1), 51–62.

37 J. Kawadkar and M. K. Chauhan, Intra-articular delivery of genipin cross-linked chitosan microspheres of flurbiprofen: Preparation, characterization, in vitro and in vivo studies, *Eur. J. Pharm. Biopharm.*, 2012, **81**(3), 563–572.

38 V. Pandit, J. M. Zuidema, K. N. Venuto, J. Macione, G. Dai and R. J. Gilbert, *et al.*, Evaluation of Multifunctional Polysaccharide Hydrogels with Varying Stiffness for Bone Tissue Engineering, *Tissue Eng., Part A*, 2013, **19**(21–22), 2452–2463.

39 M. Sarem, F. Moztarzadeh and M. Mozafari, How can genipin assist gelatin/carbohydrate chitosan scaffolds to act as replacements of load-bearing soft tissues?, *Carbohyd. Polym.*, 2012, **93**(2), 635–643.

40 M. S. Austero, A. E. Donius, U. G. K. Wegst and C. L. Schauer, New crosslinkers for electrospun chitosan fibre mats. I. Chemical analysis, *J. R. Soc., Interface*, 2012, **9**(75), 2551–2562.

41 Y. J. Hwang, J. Larsen, T. B. Krasieva and J. G. Lyubovitsky, Effect of genipin crosslinking on the optical spectral properties and structures of collagen hydrogels, *ACS Appl. Mater. Interfaces*, 2011, **3**(7), 2579–2584.

42 D. Vukajlovic, *Chitosan-Bioglass and chitosan-apatite-wollastonite composites for bone tissue engineering*, PhD thesis, Newcastle University, 2020.

43 B. Porstmann, K. Jung, H. Schmechta, U. Evers, M. Pergande and T. Porstmann, *et al.*, Measurement of lysozyme in human body fluids: Comparison of various enzyme immunoassay techniques and their diagnostic application, *Clin. Biochem.*, 1989, **22**(5), 349–355.

44 H. G. Hanstock, J. P. Edwards and N. P. Walsh, Tear Lactoferrin and Lysozyme as Clinically Relevant Biomarkers of Mucosal Immune Competence, *Front. Immunol.*, 2019, **10**, 1178.

45 A. S. Aspelund, H. Hammarström, M. Inghammar, H. Larsson, L. Hansson and B. Christensson, *et al.*, Heparin-binding protein, lysozyme, and inflammatory cytokines in bronchoalveolar lavage fluid as diagnostic tools for pulmonary infection in lung transplanted patients, *Am. J. Transplant.*, 2017, **18**(2), 444–452.

46 T. Freier, H. S. Koh, K. Kazazian and M. S. Shoichet, Controlling cell adhesion and degradation of chitosan films by N-acetylation, *Biomaterials*, 2005, **26**(29), 5872–5878.

47 X. Chen, H. Yang, Z. Zhong and N. Yan, Base-catalysed, one-step mechanochemical conversion of chitin and shrimp shells into low molecular weight chitosan, *Green Chem.*, 2017, **19**(12), 2783–2792.

48 D. M. Reynolds, *Aquatic Organic Matter Fluorescence*, Cambridge University Press, 2014, pp. 3–34.

49 K. M. Vårum, H. K. Holme, M. Izume, B. T. Stokke and O. Smidsrød, Determination of enzymatic hydrolysis specificity of partially N-acetylated chitosans, *Biochim. Biophys. Acta, Gen. Subj.*, 1996, **1291**(1), 5–15.

50 S. Dimida, A. Barca, N. Cancelli, V. D. Benedictis, M. G. Raucci and C. Demitri, Effects of Genipin Concentration on Cross-Linked Chitosan Scaffolds for Bone Tissue Engineering: Structural Characterization and Evidence of Biocompatibility Features, *Int. J. Polym. Sci.*, 2017, **2017**, 1–8.

51 F. L. Mi, Y. C. Tan, H. C. Liang, R. N. Huang and H. W. Sung, In vitro evaluation of a chitosan membrane cross-linked with genipin, *J. Biomater. Sci., Polym. Ed.*, 2001, **12**(8), 835–850.

52 F. A. Whitehead, S. A. Young and S. Kasapis, Swelling behaviour and glass transition in genipin-crosslinked chitosan systems, *Int. J. Biol. Macromol.*, 2020, **164**, 3075–3083.

53 A. Lončarević, M. Ivanković and A. Rogina, Lysozyme-Induced Degradation of Chitosan: The Characterisation of Degraded Chitosan Scaffolds, *J. Tissue Repair Regen.*, 2017, **1**(1), 12–22.

54 N. Islam, H. Wang, F. Maqbool and V. Ferro, In Vitro Enzymatic Digestibility of Glutaraldehyde-Crosslinked Chitosan Nanoparticles in Lysozyme Solution and Their Applicability in Pulmonary Drug Delivery, *Molecules*, 2019, **24**(7), 1271.

55 Q. Li, X. Wang, X. Lou, H. Yuan, H. Tu and B. Li, *et al.*, Genipin-crosslinked electrospun chitosan nanofibers: Determination of crosslinking conditions and evaluation of cytocompatibility, *Carbohydr. Polym.*, 2015, **130**, 166–174.

56 S. E. Ichi, A. Zebda, J. P. Alcaraz, A. Laaroussi, F. Boucher and J. Boutonnat, *et al.*, Bioelectrodes modified with chitosan for long-term energy supply from the body, *Energy Environ. Sci.*, 2015, **8**(3), 1017–1026.

57 M. F. Queiroz, K. R. T. Melo, D. A. Sabry, G. L. Sassaki and H. A. O. Rocha, Does the use of chitosan contribute to oxalate kidney stone formation?, *Mar. Drugs*, 2014, **13**(1), 141–158.

58 J. L. Konne, S. O. Benneth and Benneth, Synthesis and Characterization of Chitosan-Copper complex using Shells of Fresh Water Shrimps and Salt Water Crabs in Rivers State as Raw Materials, *J. Niger. Environ. Soc.*, 2014, **1**, 1–8.

59 Technology F of P and EE Lodz University of,K. Nawrotek, Z. Modrzejewska, D. Paluch, R. Zarzycki and A. Rusak, Cytotoxicity of chitosan based thermo-sensitive hydrogels intended for nervous tissue engineering, *Prog. Chem. Appl. Chitin Deriv.*, 2015, 222–235.

60 M. P. Klein, C. R. Hackenhaar, A. S. G. Lorenzoni, R. C. Rodrigues, T. M. H. Costa and J. L. Ninow, *et al.*, Chitosan

crosslinked with genipin as support matrix for application in food process: Support characterization and β-D-galactosidase immobilization, *Carbohydr. Polym.*, 2015, **137**, 184–190.

61 H. G. Sundararaghavan, G. A. Monteiro, N. A. Lapin, Y. J. Chabal, J. R. Miksan and D. I. Shreiber, Genipin-induced changes in collagen gels: Correlation of mechanical properties to fluorescence, *J. Biomed. Mater. Res., Part A*, 2008, **87A**(2), 308–320.

62 E. M. Dahmane, M. Taourirte, N. Eladlani and M. Rhazi, Extraction and Characterization of Chitin and Chitosan from Parapenaeus longirostris from Moroccan Local Sources, *Int. J. Polym. Anal. Charact.*, 2014, **19**(4), 342–351.

63 S. Mekahlia and B. Bouzid, Chitosan-Copper(II) complex as antibacterial agent: synthesis, characterization and coordinating bond-activity correlation study, *Phys. Procedia*, 2009, **2**(3), 1045–1053.

64 T. Bose, D. Latawiec, P. P. Mondal and S. Mandal, Overview of nano-drugs characteristics for clinical application: the journey from the entry to the exit point, *J. Nanopart. Res.*, 2014, **16**(8), 2527.

65 J. Reiser and M. M. Altintas, Podocytes, *F1000Research*, 2016, **5**, 114.

66 M. C. Menon, P. Y. Chuang and C. J. He, The Glomerular Filtration Barrier: Components and Crosstalk, *Int. J. Nephrol.*, 2012, **2012**, 1–9.

67 H. Pavenstädt, W. Kriz and M. Kretzler, Cell Biology of the Glomerular Podocyte, *Physiol. Rev.*, 2003, **83**(1), 253–307.

68 E. M. Renkin, Capillary transport of macromolecules: pores and other endothelial pathways, *J. Appl. Physiol.*, 1985, **58**(2), 315–325.

69 B. Rippe and B. Haraldsson, Transport of macromolecules across microvascular walls: the two-pore theory, *Physiol. Rev.*, 1994, **74**(1), 163–219.

70 W. M. Deen, C. R. Bridges, B. M. Brenner and B. D. Myers, Heteroporous model of glomerular size selectivity: application to normal and nephrotic humans, *Am. J. Physiol.*, 1985, **249**(3), F374–F389.

71 A. Remuzzi and G. Remuzzi, Glomerular perm-selective function, *Kidney Int.*, 1994, **45**(2), 398–402.

72 H. S. Choi, W. Liu, P. Misra, E. Tanaka, J. P. Zimmer and B. I. Ipe, *et al.*, Renal clearance of quantum dots, *Nat. Biotechnol.*, 2007, **25**(10), 1165–1170.

73 J. Tencer, I. M. Frick, B. W. Öquist, P. Alm and B. Rippe, Size-selectivity of the glomerular barrier to high molecular weight proteins: Upper size limitations of shunt pathways, *Kidney Int.*, 1998, **53**(3), 709–715.

74 G. D'Amico and C. Bazzi, Pathophysiology of proteinuria, *Kidney Int.*, 2003, **63**(3), 809–825.

75 P. Domalik-Pyzik, J. Chłopek and K. Pielichowska, Cellulose-Based Superabsorbent Hydrogels, *Polym. Polym. Compos. Ref. Ser.*, 2019, 1665–1693.

76 P. L. Ma, M. Lavertu, F. M. Winnik and M. D. Buschmann, New insights into chitosan-DNA interactions using isothermal titration microcalorimetry, *Biomacromolecules*, 2009, **10**(6), 1490–1499.

77 H. Zhang, Y. Li, X. Zhang, B. Liu, H. Zhao and D. Chen, Directly determining the molecular weight of chitosan with atomic force microscopy, *Front. Nanosci. Nanotechnol.*, 2016, **2**(3), 123–127.

78 W. Dong, B. Han, Y. Feng, F. Song, J. Chang and H. Jiang, *et al.*, Pharmacokinetics and biodegradation mechanisms of a versatile carboxymethyl derivative of chitosan in rats: in vivo and in vitro evaluation, *Biomacromolecules*, 2010, **11**(6), 1527–1533.

79 K. Shao, B. Han, W. Dong, F. Song, W. Liu and W. Liu, Pharmacokinetics and biodegradation performance of a hydroxypropyl chitosan derivative, *J. Ocean Univ. China*, 2015, **14**(5), 888–896.

80 N. Reviews, Glucosamine and acetylglucosamine excretion, *Nutr. Rev.*, 2009, **20**(5), 138.

81 E. Sadauskas, H. Wallin, M. Stoltenberg, U. Vogel, P. Doering and A. Larsen, *et al.*, Kupffer cells are central in the removal of nanoparticles from the organism, *Part. Fibre Toxicol.*, 2007, **4**(1), 10.

82 E. Uribe-Querol and C. Rosales, Phagocytosis: Our Current Understanding of a Universal Biological Process, *Front. Immunol.*, 2020, **11**, 1066.

83 H. H. Gustafson, D. Holt-Casper, D. W. Grainger and H. Ghandehari, Nanoparticle uptake: The phagocyte problem, *Nano Today*, 2015, **10**(4), 487–510.

84 C. Rosales and E. Uribe-Querol, Phagocytosis: A Fundamental Process in Immunity, *BioMed Res. Int.*, 2017, **2017**, 1–18.

85 J. A. Champion, A. Walker and S. Mitragotri, Role of Particle Size in Phagocytosis of Polymeric Microspheres, *J. Pharm. Res.*, 2008, **25**(8), 1815–1821.

86 T. R. Green, J. Fisher, M. Stone, B. M. Wroblewski and E. Ingham, Polyethylene particles of a "critical size" are necessary for the induction of cytokines by macrophages in vitro, *Biomaterials*, 1998, **19**(24), 2297–2302.

87 D. A. Edwards, J. Hanes, G. Caponetti, J. Hrkach, A. Ben-Jebria and M. L. Eskew, *et al.*, Large Porous Particles for Pulmonary Drug Delivery, *Science*, 1997, **276**(5320), 1868–1872.

88 K. Makino, N. Yamamoto, K. Higuchi, N. Harada, H. Ohshima and H. Terada, Phagocytic uptake of polystyrene microspheres by alveolar macrophages: effects of the size and surface properties of the microspheres, *Colloids Surf., B*, 2003, **27**(1), 33–39.

89 K. Hirota, T. Hasegawa, H. Hinata, F. Ito, H. Inagawa and C. Kochi, *et al.*, Optimum conditions for efficient phagocytosis of rifampicin-loaded PLGA microspheres by alveolar macrophages, *J. Controlled Release*, 2007, **119**(1), 69–76.

90 Y. Tabata, Y. Inoue and Y. Ikada, Size effect on systemic and mucosal immune responses induced by oral administration of biodegradable microspheres, *Vaccine*, 1996, **14**(17–18), 1677–1685.

91 Z. Sheikh, M. N. Abdallah, A. Hanafi, S. Misbahuddin, H. Rashid and M. Glogauer, Mechanisms of in Vivo Degradation and Resorption of Calcium Phosphate Based Biomaterials, *Materials*, 2015, **8**(11), 7913–7925.

92 A. Carnicer-Lombarte, S. T. Chen, G. G. Malliaras and D. G. Barone, Foreign Body Reaction to Implanted Biomaterials and Its Impact in Nerve Neuroprosthetics, *Front. Bioeng. Biotechnol.*, 2021, **9**, 622524.